Full paper/Mémoire

# Computational and experimental approaches to the molecular structure of the HCl adduct of Me$_3$PO

Andreas Orthaber, Ferdinand Belaj, Rudolf Pietschnig *

Department of Chemistry, Inorganic Section, University of Graz, Schubertstr. 1, 8010 Graz, Austria

A B S T R A C T

The reaction of anhydrous HCl$_{(g)}$ with trimethyl phosphane oxide yields trimethylhydroxy phosphonium chloride. A crystal structure analysis showed that the prevalent mesomeric structure in the solid state is the phosphonium chloride ion pair. Ab initio calculations in the gas phase cannot reproduce these findings, whereas higher correlated methods (CISD) and solvation models predict the experimental structure correctly.

© 2010 Published by Elsevier Masson SAS on behalf of Académie des sciences.

R É S U M É

La réaction du HCl$_{(g)}$ anhydre avec l'oxyde de triméthylphosphine conduit au chlorure d'hydroxytriméthylphosphonium. L'analyse par diffraction des rayons X indique que la forme prédominante est une paire ionique. Les approches DFT en phase gazeuse ne permettent pas de retrouver la structure déterminée à l'état cristallin, alors que les méthodes plus hautement corrélées CISD ainsi que des modèles de solvatation reproduisent la structure expérimentale.

© 2010 Published by Elsevier Masson SAS on behalf of Académie des sciences.

## 1. Introduction

The bonding situation in different phosphanes, phosphane oxides, and ylides has been investigated over the last decades [1–3]. Earlier investigations of differently substituted formal "hydroxy phosphonium halides" showed the influence of the counter ion with respect to the contributions of the mesomeric structures 1,2 and their isomer 3 (Scheme 1). The corresponding triphenyl substituted phosphonium cation was studied crystallographically with different formal counter ions, like for e.g. F⁻, [4], Cl⁻ [5], Br⁻

[6], H$_2$O*Br⁻ [7]. For X = F the best description is formula **1**, which can be attributed to the strong H–F bond. For the softer atoms (X = Cl and Br), which are also weaker bases, the crystal structures revealed the corresponding hydroxytriphenyl phosphonium halides **(2)** as the prevalent tautomeric structure. For X = Br also, the formation of a water adduct (type **4**) was observed. Whereas the phenyl substituted phosphonium compounds have been studied extensively, only little is known about their aliphatic congeners. Some earlier spectroscopic results from NMR and IR investigations suggested, however, a similar trend for the aliphatic compounds [8]. Nevertheless, only a single crystal structure with trialkyl substitution was reported in the literature, so far (type **2**: R = $^i$Pr, X = I) [9], and a further compound having an indenyl and two methyl substituents

* Corresponding author.
  E-mail address : rudolf.pietschnig@uni-graz.at (R. Pietschnig).
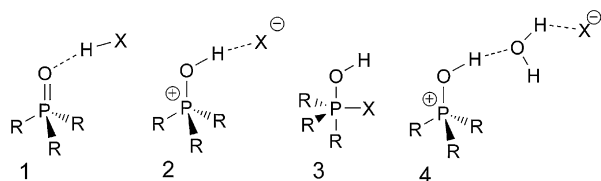
Scheme 1. Isomeric structures of hydrogen halide adducts of oxophosphoranes 1–3, including a water containing variety (4).



Scheme 2. Synthesis of 5 starting from trimethyl phosphane oxide (6) or the chlorotrimethyl phosphonium chloride (7).

in the form of its water adduct (type 4: X = Cl) [10]. By contrast, the *soft–soft* interactions of various iodo-phosphonium salts with iodine (I⁻, I₃⁻) have been studied extensively [9,11–13]. In our work, we wanted to investigate the bonding situation of adducts of hydrogen halides with the smallest trialkyloxophosphorane, *i.e.* trimethyl phosphane oxide.

## 2. Results and discussion

In order to get insight into the bonding situation of the alkyl substituted compounds $R_3POHX$, we performed an exploratory *ab initio* study on the simplest representatives (R=CH₃, X = F, Cl, Br). Our initial attempts to analyze these molecules by means of DFT calculations (B3LYP) with a triple ζ basis set (6–311G**) revealed that only the bromine derivative exists as a type 2 structure. We attributed these findings to the incompleteness of the basis set not able to describe diffuse electron distribution. Addition of diffuse functions (B3LYP/6-311++G**) did not alter the findings. The fluorine and the bromine derivatives show the phosphane oxide adduct (2) and the phosphonium ion (1), respectively. A summary of selected geometric parameters is given in Table 1. Nevertheless, the PO bond lengths for the fluorine derivative (1.513 Å) is significantly longer than for trimethylphosphane oxide (1.489(6) Å [14] and 1.500 Å) suggesting some interaction between the P=O and the HF moiety.[1] Interestingly, for the chlorine derivative, the calculations also predict the HCl adduct rather than the phosphonium ion as the minimum energy structure. Interaction of the HCl molecule with trimethylphosphane oxide results in a stabilization by ca. 3.2 kcal/mol ($\Delta G_{interaction}$). Only the bromine derivative shows the expected phosphonium ion structure having a shortened O–H (1.069 Å) and elongated H–Br (1.935 Å) distance.

This is, in fact, the opposite of the experimental findings with R = phenyl. It seems, however, very unlikely that changing phenyl to alkyl substituents would switch the preferred structure from type 2 to 1. Therefore, we synthesized this compound to check the bonding situation experimentally. General access to phosphonium halides is given by reaction of the phosphane oxide 6 with the corresponding anhydrous HX. We were also able to obtain
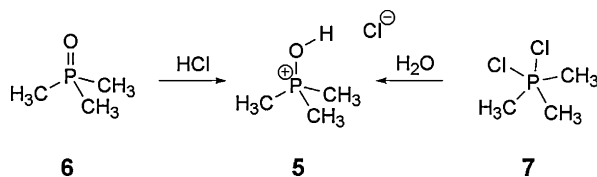
5 after gentle hydrolysis of 7 [15] (Scheme 2). In the ³¹P NMR spectra, a signal at +66.9 ppm is observed. This is in good agreement with similar compounds [16]. The proton spectra show one doublet at 1.93 ppm ($^3J_{PH}$ = 18 Hz) and a broad singlet at 8.74 ppm. In the ¹³C NMR spectra, a doublet at 15.53 ppm (d, $^1J_{PC}$ = 91.6 Hz) is observed. Based on the spectroscopic data, the presence of the pentavalent isomer 3 seems unlikely; however, no unambiguous assignment between the remaining possible isomeric structures 1 and 2 can be made.

We were also able to grow single crystals suitable for X-ray diffraction from a saturated chloroform solution. The crystal structure analysis clearly shows the formation of a hydroxytrimethyl phosphonium chloride. All atoms are on general positions. All non-hydrogen atoms are refined with anisotropic displacement parameters, while the hydrogen atoms were refined isotropically without any geometric constraints. The hydrogen bond [O1–H1···Cl1 179.5(14)°, O1···Cl1 2.8763(4) Å] connects the ion pair which shows almost $C_s$ symmetry. The chloride anion is surrounded by two methyl groups and the next oxygen atom is as near as 3.7421(5) Å having no significant contributions to the stabilization of the phosphonium ion pairs. Interestingly, the P–O bond is very short (P1–O1 1.5600(4) Å), which is only 4.7% longer than in Me₃P=O (Fig. 1).

In order to account for the observed discrepancy of the calculated and the X-ray structure, we tried to involve the surroundings of the molecule in a very simple way. The very common IEF-PCM formalism for modeling a solvent by means of a polarizable continuum was used to mimic the crystallographic surroundings. For these calculations, one needs to specify a "solvent" by its dipole moment ($\mu$) and the mean polarizability ($\bar{\alpha}$). Those parameters were obtained from preliminary calculations of the phosphonium ion in a highly polar medium modeled by the IEF-PCM[2] using the Onsager equation (Eq. (4)) for polar liquids. Accounting for the different orientations of the dipole moment in the solid state gives the Kirkwood correlation factor. By using this approach, we were able model the observed structure. Interestingly also a higher correlated method – CISD – showed good agreement with the X-ray structure, but not 2nd and 3rd order Møller-Plesset calculations (MP2, and MP3). Table 2 gives relevant

---

[1] The P=O bond lengths from our calculations and the X-ray structural analysis show very good agreement, though. Also the experimental P=O stretching mode (1163 cm⁻¹) is in accordance with scaled/unscaled DFT results (1158/1206 cm⁻¹) with a scaling factor of 0.96.

[2] The continuum model IEF-PCM was used with standard parameters for water. Owing to the fact that cavities are formed as spheres over the heavy atoms only and hydrogen atoms are supposed to lie in these spheres, we used the universal force field (UFF) cavity formation algorithm.

**Table 1**

Structural changes on adduct formation. Comparison of selected geometric parameters of $(CH_3)_3POHX$ (calculated) with $(CH_3)_3PO$ (calculated and experimental). Distances in [Å] and angles in [°].

| $(CH_3)_3POHX$ | | | | $(CH_3)_3PO$ | |
|---|---|---|---|---|---|
| X = | F | Cl | Br | – | – |
| | | B3LYP/6-311++G(d,p) | | B3LYP/6-311++G(d,p) | X-ray [14] |
| P–O | 1.513 | 1.512 | 1.568 | 1.500 | 1.489(6) |
| P–C$_{trans}$ | 1.821 | 1.822 | 1.807 | 1.830 | 1.772(6) |
| P–C$_{cis}$ | 1.823 | 1.823 | 1.808 | 1.830 | 1.772(6) |
| O–H | 1.581 | 1.619 | 1.069 | – | – |
| O…X | 2.534 | 2.960 | 2.973 | – | – |
| H–X | 0.959 | 1.344 | 1.935 | – | – |
| C–P–OH | 10.0 | 34.1 | 180.0 | – | – |
| POX | 121.7 | 127.5 | 99.4 | – | – |
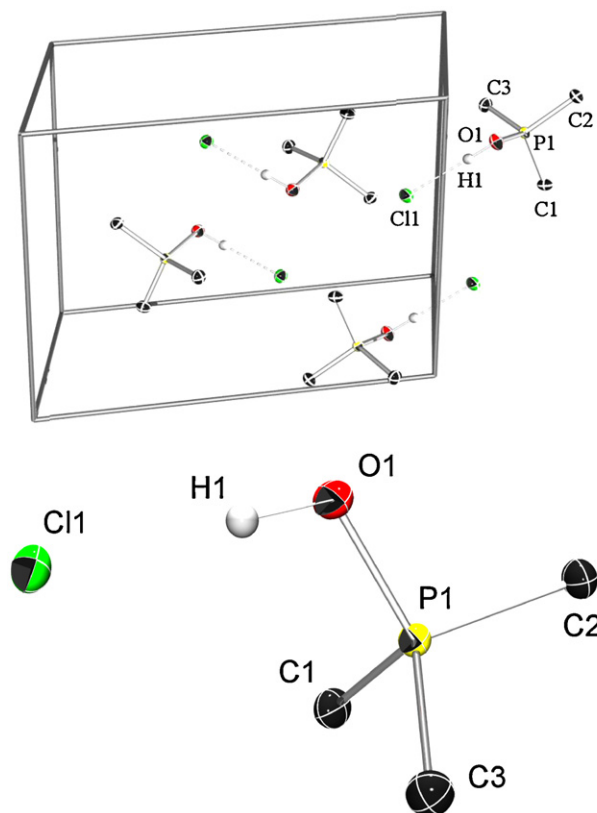


**Fig. 1.** ORTEP plot of the unit cell content of **5** showing the four nearest molecules. Probability level of the thermal ellipsoids is 50%, hydrogen atoms are drawn at arbitrary radii. The hydrogen bond of the ion pairs is displayed with dotted lines. Selected distances [Å] and angles [°]: P1–O1 1.5600(4), P1–C1 1.7740(5), P1–C2 1.7725(5), P1–C3 1.7798(6), O1–H1 0.90(1), H1–Cl1 1.98(1), O1–H1···Cl1 179.5(14).

structural parameters of the calculated and the X-ray structures.

A detailed analysis of the molecular orbitals of trimethyl phosphine oxide (**6**) and **5** at the B3LYP/6-311++G** level of theory with IEF-PCM ($\varepsilon_R = 98$ and $r_{solv.} = 5.32$ Å) was carried out in order to understand the rather short P–O single bond. In **6** the s-type orbitals at the oxygen and phosphorus atoms form a highly polarized σ-bond (Fig. 2 a) and two p-type lone pairs of O show significant negative hyperconjugation with the P–C antibonding orbitals (Fig. 2 b + c)

resulting in a short P–O bond. In compound **5**, the two σ-bonds (P–O and O–H) form two linear combinations ($\sigma_{O-H} + \sigma_{P-O}$ (d) and $\sigma_{O-H} - \sigma_{P-O}$), with less polarization towards the oxygen atom compared to **6**. Furthermore, the p-type orbitals of the oxygen atom show slightly diminished, but still significant negative hyperconjugation (Fig. 2 e + f). Interestingly, the interaction energy in **5** gives similar results for the solvation models ($\Delta G_{interaction}$ 3.9 kcal/mol) and the gas phase ($\Delta G_{interaction}$ 3.2 kcal/mol) despite their significantly different structures.

**Table 2**
Comparison of calculated and measured structural parameters of Me₃POHCl.

| g.p[b]./PCM[c] | X-ray | B3LYP 6–311G** | 6–311++G** | 6–311++G** PCM: 0.5 | PCM: 80 | PCM: 98 | CISD 6–311++G** | MP2 6–311++G** | MP3[a] 6–311++G** |
|---|---|---|---|---|---|---|---|---|---|
| | | g.p. | g.p. | | | | g.p. | g.p. | g.p. |
| P–O | 1.560(1) | 1.512 | 1.515 | 1.507 | 1.585 | 1.590 | 1.547 | 1.515 | 1.497 |
| P–C$_{trans}$ | 1.780(1) | 1.822 | 1.823 | 1.825 | 1.796 | 1.795 | 1.791 | 1.821 | 1.812 |
| P–C$_{cis}$ | 1.773(1) | 1.823 | 1.821 | 1.826 | 1.803 | 1.802 | 1.791 | 1.823 | 1.811 |
| O···H | 0.897(14) | 1.619 | 1.615 | 1.709 | 1.024 | 1.020 | 1.041 | 1.615 | 1.686 |
| O···Cl | 2.876(1) | 2.960 | 2.580 | 3.020 | 2.916 | 2.931 | 2.787 | 2.958 | 2.989 |
| H–Cl | 1.979(14) | 1.344 | 1.346 | 1.331 | 1.892 | 1.912 | 1.779 | 1.346 | 1.309 |
| C–P–O–H | −176.7(9) | −145.9 | −172.0 | 178.3 | −179.7 | 179.9 | 180.0 | 171.9 | −0.1 |
| P–O–Cl | 113.6(1) | 127.5 | 125.9 | 111.5 | 114.4 | 115.3 | 98.2 | 123.4 | 128.5 |
| rmsd (dist)[d] | – | 0.40 | 0.41 | 0.43 | 0.07 | 0.06 | 0.11 | 0.39 | 0.43 |
| rmsd (ang)[e] | – | 23.9 | 9.3 | 1.9 | 2.2 | 2.6 | 11.2 | 7.7 | 125.3 |

[a] Calculations resulted in a staggered orientation of the C–P–O–H moiety.
[b] Gas phase calculations.
[c] Solvation model IEF-PCM with respective permittivity and $r_{solv.}$ = 5.32 Å.
[d] Root mean square deviation (rmsd) of selected distances [Å].
[e] rmsd of selected angles [°].
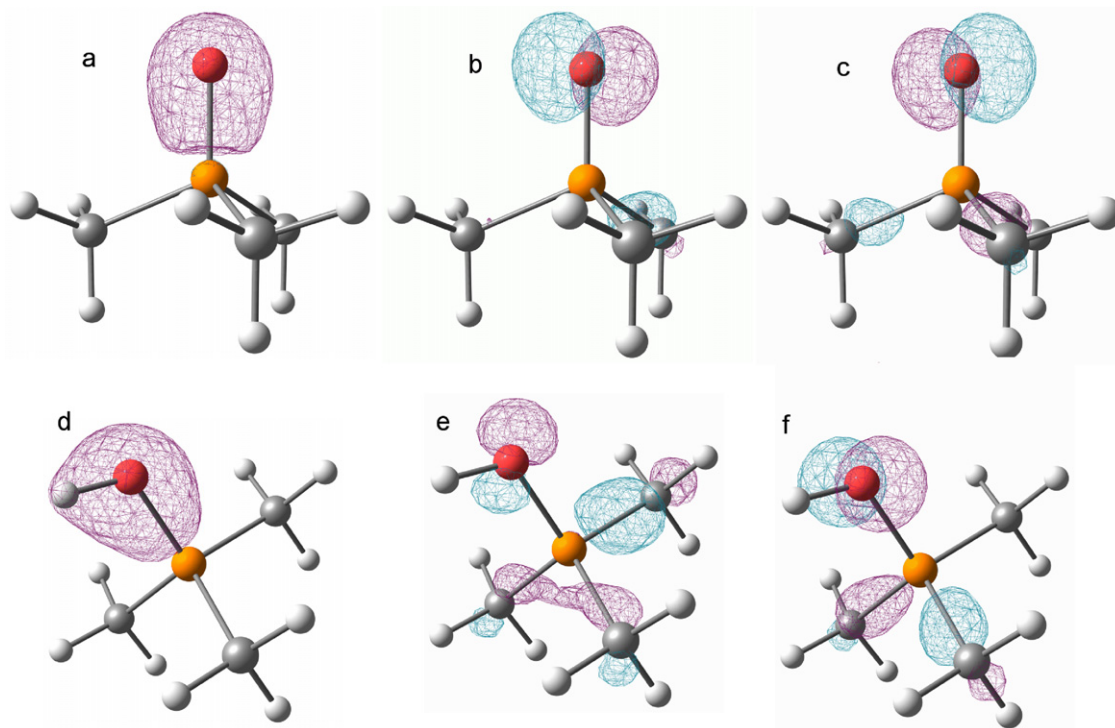


Fig. 2. Graphical representation of selected molecular orbitals for **6** (top a–c) and **5** (bottom (d–f) at a contour level of 0.1 a.u. a: HOMO-15. b: HOMO-1. c: HOMO. d: HOMO-19. e: HOMO-4. f: HOMO-3.

## 3. Conclusion

We were able to synthesize and structurally characterize the hydroxymethyl phosphonium chloride, which proves the presence of distinct ion pairs in the solid state. Different calculations referring to gas phase, solution, and "solid" state reveal a large influence of the molecular surroundings on the bonding situation besides the counter-ion which plays a crucial role for the prevailing structural isomer of these compounds. Widely implemented continuum models like the PCM were used to model the environment in the solid state for an easy prediction and confirmation of the solid state structure.

## Appendix A. Computational details

All *ab initio* calculations have been carried out with the Gaussian G03 (Rev. B.04) suite of programs. All structures were fully optimized and their frequency analysis showing no imaginary frequency. The Debye-Clausius-Mosotti equation can be used for the evaluation of permittivity of molecules with a negligible permanent dipole moment. Limitations of this theory are caused by neglecting the contribution of changing the electric field induced by the permanent dipole moment:

$$\frac{\varepsilon_R - 1}{\varepsilon_R + 2} = \frac{\rho}{M} \frac{N_A}{3\varepsilon_0} * \left( \bar{\alpha} + \frac{\bar{\mu}^2}{3 * k * T} \right) \tag{1}$$

One of the first modifications to this theory was given by Onsager, who introduced the term "reaction field" (Eqs. (2), (3)). In brief, this is the response of the external dielectric to the dipole moment of the solute. This methodology also proved successful also for the calculation of relative permittivities of polar liquids.

$$\varepsilon_0(\varepsilon_R - 1) = N_1 \frac{3\varepsilon_R}{2\varepsilon_R + 1} * \frac{1}{1 - \bar{\alpha} f_R} * \left( \bar{\alpha} + \frac{1}{1 - \bar{\alpha} f_R} * \frac{\mu^2}{3kT} \right),$$
where $\tag{2}$

$$f_R = {}^2/_3 * {}^{N_1}/_{\varepsilon_0} * {}^{\varepsilon_R-1}/_{2\varepsilon_R+1} \tag{3}$$

This approach does not account for dipole–dipole interactions. To include these interactions quantitatively, Kirkwood introduced a simple scaling factor $G_K$ which reduces the molecular dipole moment to the effective dipole moment ($G_K * \mu_{mol.} = \mu_{eff.}$). This factor is defined as: $G_K = 1 + \frac{1}{n}\sum_n \cos(\varphi_n)$, where $n$ is the number of direct neighbors and $\varphi_n$ the angle enclosed by their respective dipole moment. For the case that the $G_K$ factor becomes one, the Kirkwood equation (4) equals the Onsager equation (2).

$$\varepsilon_0(\varepsilon_R - 1) = N_1 \frac{3\varepsilon_R}{2\varepsilon_R + 1} * \frac{1}{1 - \bar{\alpha} f_R} * \left( \bar{\alpha} + \frac{1}{1 - \bar{\alpha} f_R} * \frac{G_K \mu^2}{3kT} \right), \tag{4}$$

In order to determine an approximate Kirkwood factor for the crystal state, we used the dipole moment vector obtained from preliminary calculations. By alignment of the molecules (only heavy atoms) from the calculations and the X-ray structure, we obtained a translation (center of masses) and rotation matrix. The respective rotation matrices were then used to transform the computed dipole moment and calculate the angles between the different orientations in the solid state. The average of the four nearest different orientations was used to calculate the Kirkwood factor ($G_K = 0.1412$).

Solving Eq. (3) with respect to $\varepsilon_R$ gives, in general, three solutions (one imaginary, one real negative and one positive solution, which is the physically meaningful one). The permittivity for the PCM calculations has been updated only three times showing already good conver-

gence ($\varepsilon_R = 98$). The radius of the "solvent sphere" was estimated by taking the volume of the unit cell as determined from the X-ray structure divided by the number of molecules present in the cell and transforming it to a spherical shape.

## Appendix B. Synthesis of *5*

All reactions were carried out under argon using modified Schlenk techniques. NMR spectra were recorded on a Varian UnityInova operating at a proton frequency of 400 MHz at 25 °C. Mass spectrometry was performed on an Agilent 5975C mass spectrometer equipped with a direct injection unit (DI-EI).

Compound **5** was synthesized according to a published procedure [8] bubbling anhydrous $HCl_{(g)}$ through a suspension of $OPMe_3$ (6.0 mmol, 0.55 g) in 100 ml $Et_2O$. After filtration and removal of the solvent under reduced pressure, **5** is obtained in reasonable yields (67%, 0.52 g, 4.0 mmol). $^1H(CDCl_3, 400\ MHz)$: 1.93 ppm ($^3J_{PH}$ = 18 Hz). $^{13}C(CDCl_3, 100\ MHz)$: 15.53 ppm ($d$, $^1J_{PC}$ = 91.6 Hz). $^{31}P(CDCl_3, 121\ MHz)$: 66.9 ppm. EI-MS (m/z): 128.1/130.1 $M^+$ (42); 92.1 $Me_3PO^+$ (85); 77.1 $Me_3PO^+$-$CH_3$ (100).

## Appendix C. Crystallographic details

The crystal structure of **5** was determined with a Bruker APEX-II CCD diffractometer using graphite-monochromatized Mo $K_\alpha$ radiation at 100 K. The structure was solved and refined using the SHELXL and SHELXS suite of programs [17,18]. Structure plots have been prepared using ORTEP [19]. Supplementary crystallographic data for this article can be obtained free of charge quoting CCDC 761598 from The Cambridge Crystallographic Data Centre via www.ccdc.cam.ac.uk/data_request/cif.

| *Crystal data* | |
|---|---|
| Empirical formula | $C_3H_{10}OP^+Cl^-$ |
| Formula weight | 128.53 |
| Crystal description | Block, colorless |
| Crystal size | $0.28 \times 0.28 \times 0.18$ mm |
| Crystal system, space group | Monoclinic, P $2_1/n$ |
| Unit cell dimensions | |
| a | 6.3264(2) Å |
| b | 9.1397(3) Å |
| c | 11.3681(4) Å |
| β | 105.8420(10) ° |
| Volume | 632.35(4) Å$^3$ |
| Z | 4 |
| Calculated density | 1.350 Mg/m$^3$ |
| F(000) | 272 |
| Linear absorption coefficient μ | 0.735 mm$^{-1}$ |
| Absorption correction | Semi-empirical from equivalents |
| Max. and min. transmission | 0.748 and 0.643 |
| Unit cell determination | $2.90 < \Theta < 40.67°$ |
| | 6625 reflections used at 100K |
| *Data collection* | |
| Radiation source | Fine-focus sealed tube |
| Radiation and wavelength | MoK$_\alpha$, 0.71073 Å |

| | |
|---|---|
| Scan type | φ and ω scans |
| Θ range for data collection | 3.36 to 40.00° |
| Index ranges | $-11 \leq h \leq 11$, |
| | $-15 \leq k \leq 16$, $-15 \leq l \leq 20$ |
| Reflections collected/unique | 10607/3906 |
| Significant unique reflections | 3507 with $I > 2\sigma(I)$ |
| R(int), R(sigma) | 0.0177, 0.0194 |
| Completeness to $\Theta = 40.0°$ | 99.4% |

*Refinement*

| | |
|---|---|
| Refinement method | Full-matrix least-squares on $F^2$ |
| Data/parameters/restraints | 3906/95/0 |
| Goodness-of-fit on $F^2$ | 1.052 |
| Final R indices [$I > 2\sigma(I)$] | R1 = 0.0211, wR2 = 0.0568 |
| R indices (all data) | R1 = 0.0245, wR2 = 0.0585 |
| Extinction expression | None |
| Weighting scheme | $w = 1/[\sigma^2(F_o^2) + (aP)^2 + bP]$ |
| | where $P = (F_o^2 + 2F_c^2)/3$ |
| Weighting scheme parameters $a, b$ | 0.0315, 0.0495 |
| Largest $\Delta/\sigma$ in last cycle | 0.001 |
| Largest difference peak and hole | 0.437 and $-0.356 e/\text{Å}^3$ |

## Appendix D. Supplementary data

Supplementary data associated with this article can be found, in the online version, at doi:10.1016/j.crci.2010.07.006.

## References

[1] D.G. Gilheany, Chem. Rev. 94 (1994) 1339.
[2] T. Malaspina, L.T. Costa, E.E. Fileti, Int. J. Quantum Chem. 109 (2009) 250.
[3] J.A. Dobado, H. Martinez-Garcia, J.M. Molina, M.R. Sundberg, J. Am. Chem. Soc. 120 (1998) 8461.
[4] D. Thierbach, F. Huber, Z. Anorg. Allg. Chem. 451 (1979) 137.
[5] H.J. Haupt, F. Huber, C. Krüger, H. Preut, D. Thierbach, Z. Anorg. Allg. Chem. 436 (1977) 229.
[6] H.P. Lane, C.A. McAuliffe, R.G. Pritchard, Acta Crystallogr., Sect. C: Cryst. Struct. Commun. 48 (1992) 2002.
[7] D. Thierbach, F. Huber, Z. Anorg. Allg. Chem. 457 (1979) 189.
[8] V.V. Malovik, V.Y. Seminii, V.N. Zavatskii, I.E. Boldeskul, N.N. Kalibab-chuk, E.V. Ryl'tsev, Russ. J. Gen. Chem. 47 (1977) 1017.
[9] F. Ruthe, P.G. Jones, W.W. du Mont, P. Deplano, M.L. Mercuri, Z. Anorg. Allg. Chem. 626 (2000) 1105.
[10] D.N. Kazul'kin, A.N. Ryabov, V.V. Izmer, A.V. Churakov, I.P. Beletskaya, C.J. Burns, A.Z. Voskoboynikov, Organometallics 24 (2005) 3024.
[11] V. Stenzel, J. Jeske, W.-W. du Mont, P.G. Jones, Inorg. Chem. 34 (1995) 5166.
[12] W.W. du Mont, F. Ruthe, Coord. Chem. Rev. 189 (1999) 101.
[13] W.I. Cross, S.M. Godfrey, C.A. McAuliffe, R.G. Pritchard, J.M. Sheffield, G.M. Thompson, J. Chem. Soc., Dalton Trans. (1999) 2795.
[14] L. Engelhardt, C. Raston, C. Whitaker, A. White, Aust. J. Chem. 39 (1986) 2151.
[15] A. Orthaber, F. Belaj, R. Pietschnig, J. Organomet. Chem. 695 (2010) 974.
[16] M.M. Crutchfield, C.H. Dungan, J.H. Letcher, V. Mark, J.R. Van Wazer, [31]P Nuclear Magnetic Resonance, Vol. 5, Interscience Publishers, New York, 1967
[17] G.M. Sheldrick, SHELXL-97. Program for the Refinement of Crystal Structures, University of Göttingen, Germany, 2008.
[18] G.M. Sheldrick, SHELXS-97. Program for the Solution of Crystal Structures, University of Göttingen, Germany, 2008.
[19] L.J. Farrugia, J. Appl. Cryst. 30 (1997) 565.